Current Optics and Photonics
Vol. 3, No. 4, August 2019, pp. 304-310

ISSN: 2508-7266(Print) / ISSN: 2508-7274(Online)
DOI: https://doi.org/10.3807/COPP.2019.3.4.304

Design of a Polarization Splitter Based on a Dual-core Hexagonal-shaped Photonic Crystal Fiber

Subramani Jegadeesan[1]*, Muneeswaran Dhamodaran[1], Maria Azees[2], and Arunachalam Murugan[1]

[1]*M.Kumarasamy College of Engineering, Karur 639113, Tamilnadu, India*
[2]*GMR Institute of Technology, Rajam 532127, Andra Pradesh, India*

(Received December 21, 2018 : revised January 30, 2019 : accepted May 31, 2019)

In this paper, a microstructured, hexagonal-shaped dual-core photonic crystal fiber (PCF) is proposed. The proposed structure has specific optical properties to obtain high birefringence and short coupling length, for different values of structural parameters varied over a wide range of wavelength. The properties are analyzed using a solid core of silica material. The proposed structure is implemented as a polarization splitter with splitting length of 1.9 mm and a splitting ratio of -34.988 dB, at a wavelength of 1550 nm. The obtained bandwidth in one band gap of about 81 nm. The numerical analysis ensures that the performance of the proposed polarization splitter is better than that of existing ones.

Keywords : Photonic crystal fiber, Hexagonal-shaped, Birefringence, Coupling length, Polarization splitter
OCIS codes : (060.2340) Fiber optics components; (060.2420) Fibers, polarization-maintaining

I. INTRODUCTION

Photonic crystal fiber (PCF) is a new type of micro-structured optical fiber that consists of small, closely packed air holes. It is produced using the stack-and-draw method. In the PCF, light is confined inside the silica tubes. Special properties of PCF have attracted a number of researchers in recent years. [1-3] introduced a new type of fiber to carry the light signal in a hollow core by means of photonic band-gap cladding. [4] proposed another type of PCF with a cladding structure with periodic air holes in silica. The main parameters considered in designing a PCF are the diameter d of air holes and the distance between the centers of two adjacent air holes D, which is shown in Fig. 1. The PCF coupler is one of the key elements in advanced optical networks [5-9].

Compared to conventional optical couplers, PCF provides significant features such as flexible dispersion, high nonlinearity, and support for single-mode transmission. Realization of dual-core PCF allows us to design efficient PCF couplers, wavelength multiplexers, de-multiplexers, splitters, filters, and sensors [10-14]. Dual-core PCF couplers have numerous advantages over conventional optical couplers and are more flexible to design, easy to make, and present a shorter coupling length. The important physical properties of dual-core PCF are the coupling length and birefringence [15-19].

The main objective of this work is to analyze the physical properties of the dual-core hexagonal-shaped PCF

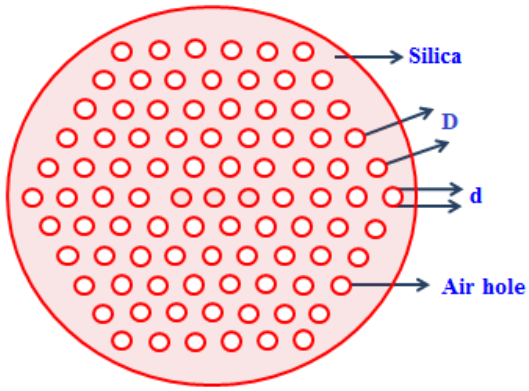

FIG. 1. Photonic crystal structure.

*Corresponding author: jegadeesans@rediffmail.com, ORCID 0000-0002-6457-4906
Color versions of one or more of the figures in this paper are available online.

This is an Open Access article distributed under the terms of the Creative Commons Attribution Non-Commercial License (http://creativecommons.org/licenses/by-nc/4.0/) which permits unrestricted non-commercial use, distribution, and reproduction in any medium, provided the original work is properly cited.

Copyright © 2019 Current Optics and Photonics

to achieve high birefringence and short coupling length for different values of structural parameters, and that the proposed structure is designed to be implemented as a polarization splitter.

II. PROPOSED DUAL-CORE HEXAGONAL-SHAPED PCF DESIGN

2.1. Physical Structure

The physical structure of dual-core PCF is shown in Fig. 1. The important structural parameters of our proposed structure are d the diameter of the air holes, and the pitch D, which is the distance between two adjacent air holes in the cladding. In our proposed structure, d is 1.4 μm, while D is 2.2 μm. The refractive index of air hole $n_d = 1$. Here silica is used as a background material with a refractive index of $n_{si} = 1.45$. A dual-core hexagonal-shaped PCF is designed by eliminating the two air holes on both sides of the middle air hole in parallel lines. Hence, asymmetry is introduced in the structure, which creates high birefringence and short coupling length. The proposed structure is designed to be implemented as a polarization splitter. Different properties of PCF are analyzed by changing the value of d in the air holes in the cladding for d/D values of 0.5, 0.6, 0.7, 0.8, and 0.9. The properties are analyzed using a solid core of silica material. The proposed polarization splitter's structure is shown in Fig. 2.

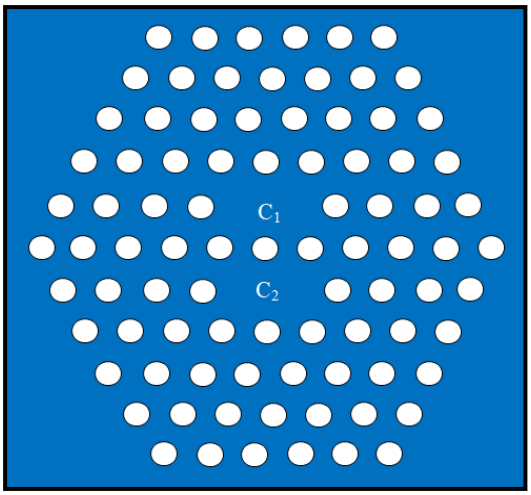

FIG. 2. Dual-core hexagonal-shaped photonic crystal fiber.

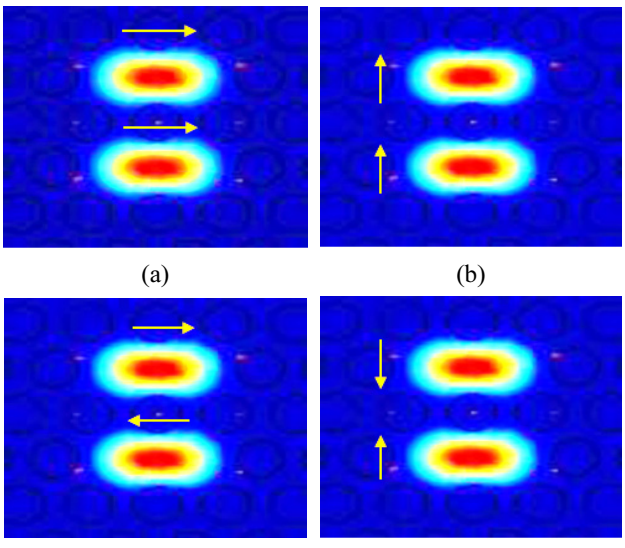

FIG. 3. Simulated structure of dual core hexagonal-shaped PCF: (a) x-polarized (even mode), (b) y-polarized (even mode), (c) x- polarized (odd mode), (d) y-polarized (odd mode).

The dual-core hexagonal PCF structure is designed by varying the structural parameters D and d and simulated using the finite-element method (FEM). Figure 3 shows the simulation results for the proposed PCF structure. It shows the light confinement in the x- polarized direction at a wavelength of 1.55 μm. Also, it shows the four different supermodes, and explains the field distribution in the fiber core.

2.2. Band Gap Calculation

Maxwell's equations are used to study electromagnetic wave propagation in the photonic crystal structure. Maxwell's third and fourth equations in the magnetic field form is given by

$$\nabla \times \left(\frac{1}{\varepsilon(\vec{r})} \nabla \times H(\vec{r})\right) = \left(\frac{\omega}{c}\right)^2 H(\vec{r}) \tag{1}$$

where ω is the angular frequency, c is the speed of light in vacuum, and $\varepsilon(r)$ is the relative permittivity of the material.

Let us assume that the two-dimensional photonic crystal system is periodic in the x and y directions and homogeneous in the z direction. The modes in photonic crystals are categorized into two polarizations, as the TM mode and TE mode. For the TE mode the magnetic field is along the z direction ($\vec{H} = H_z \vec{a}_z$), and for the TM mode the electric field along the z direction ($\vec{E} = E_z \vec{a}_z$).

To calculate the band gap, quadratic eigenvalue calculations are made over a unit cell of the photonic crystal lattice with Floquet periodic boundary conditions. We optimize the structural parameters of the PCFs and use the plane-wave method to calculate the band gap of the band-gap-guiding PCFs, and FEM to model all of the properties. The band gap, index-guiding mode line, the x and y-polarized guiding mode lines, and the cladding line are shown in Fig. 4 for the values of $n_d = 1$, $n_{si} = 1.45$, $d = 1.4$ μm and $D = 2.2$ μm.

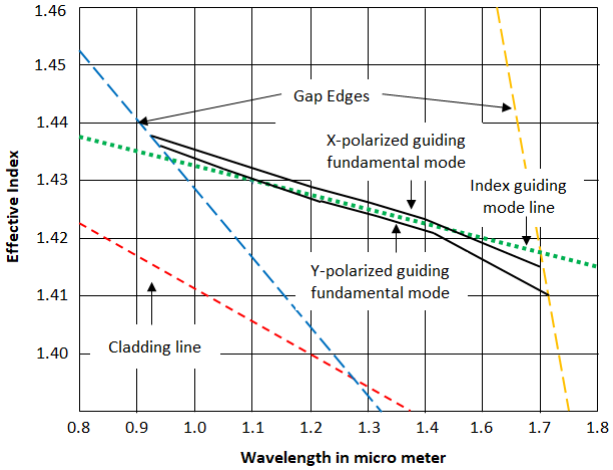

FIG. 4. Modal effective indices of the two polarized fundamental modes and band-gap map, as a function of wavelength.

III. ANALYSIS OF OPTICAL PROPERTIES OF DUAL-CORE HEXAGONAL-SHAPED PCF

3.1. Effective Index

The refractive index of the proposed structure in PCFs exhibits a strong wavelength dependence, very different from pure silica, which allows PCFs to be designed with a new set of features unattainable within the classical approach. Figure 5 shows that when the wavelength is increased, the value of the effective index decreases and is shown in quasi-TE for the even supermode. Effective index for different *d/D* decreases as wavelength increases. For smaller wavelengths, the light confinement is strong and the effective index value is high, but at higher wavelengths the effective index value decreases. At 1.55 μm, the effective index is reduced as the *d/D* ratio is increases. Table 1 shows the effective index for different *d/D* at 1.55 μm.

3.2. Birefringence

Birefringence is defined as the difference between the propagation constants or mode indices of the slow and fast polarization modes. Birefringence is the difference between the mode indices of the orthogonally polarized modes:

$$B = \left| \mathrm{Re}(n_{ei}^{x}) - \mathrm{Re}(n_{ei}^{y}) \right| \tag{2}$$

where n_{ei}^{x} and n_{ei}^{y} are effective indices in the *x*-polarized and *y*-polarized directions respectively. From Fig. 6, it is observed that the birefringence increases at higher wavelengths when the size of each air hole increases. Hence, at a wavelength of 1.55 μm the birefringence increases as the *d/D* value is increased. High birefringence is obtained due to the asymmetric structure. Birefringence curves are shown for the even supermode.

For all *d/D* values, the birefringence is found to be of the order of 10^{-3} at 1.55 μm. Table 2 shows the obtained birefringence for different *d/D* values at 1.55 μm.

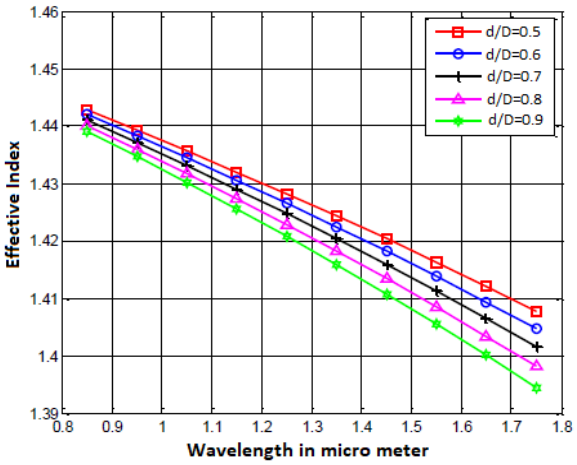

FIG. 5. Effective index varying with wavelength, for different *d/D* ratios.

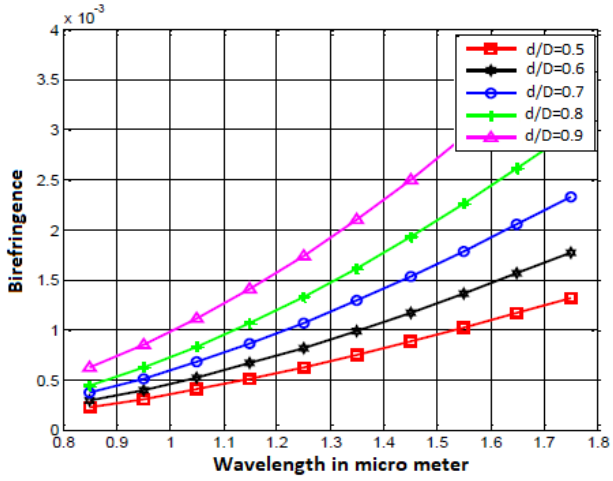

FIG. 6. Birefringence variying with wavelength, for different *d* and constant *D* values.

TABLE 1. Effective index for different *d/D* at 1.55 μm

Effective index at 1.55 μm				
d/D = 0.5	*d/D* = 0.6	*d/D* = 0.7	*d/D* = 0.8	*d/D* = 0.9
1.420013	1.419937	1.409849	1.405734	1.401371

TABLE 2. Birefringence for different *d/D* at 1.55 μm

Birefringence at 1.55 μm				
d/D = 0.5	*d/D* = 0.6	*d/D* = 0.7	*d/D* = 0.8	*d/D* = 0.9
1.109×10^{-3}	1.293×10^{-3}	1.802×10^{-3}	2.191×10^{-3}	2.894×10^{-3}

3.3. Coupling Length

In accordance with mode-coupling theory, the even and odd supermodes describe the coupling length of a dual-core fiber. Modes of an individual core having symmetric field distribution make even supermodes, and modes of an individual core having asymmetric field distribution make odd super modes. The dual-core PCF coupling length is defined as

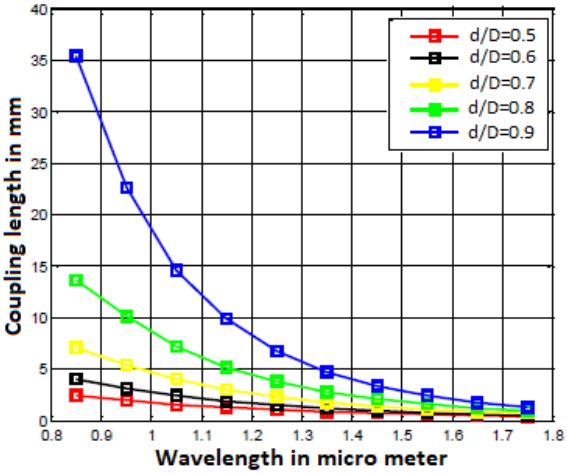

FIG. 7. Coupling length for *x*-polarized light, changing with wavelength.

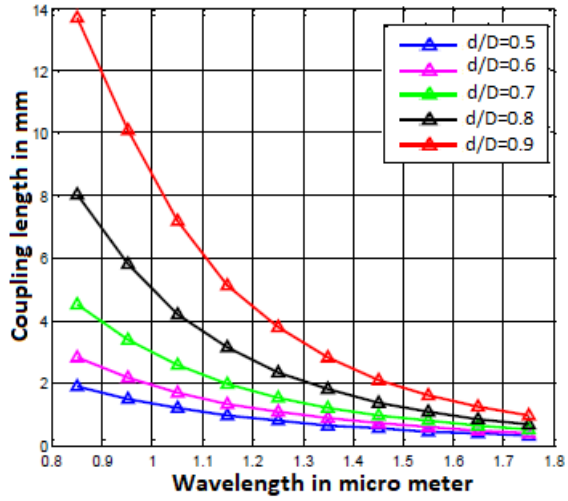

FIG. 8. Coupling length for *y*-polarized light, changing with wavelength.

$$L_c = \frac{\pi}{k_e^p - k_o^p} = \frac{\pi}{2(n_e^p - n_o^p)}, p = x, y \tag{3}$$

where n_e^p and n_o^p are the *p*-polarized even and odd supermodes' effective indices. k_e^p and k_o^p are the propagation constants of *p*-polarized even and odd supermodes. The fiber's coupling length depends on the structure of the PCF. Equation 3 explains the coupling-length calculation for *x*- and *y*-polarized light. The dual-core hexagonal-shaped PCF structure has a better coupling length for larger *d/D* values. When the wavelength increases, the proposed dual-core hexagonal-shaped PCF gives a small coupling-length. If the length of the coupling is very small, then a small length coupler or splitter can be realized. Figs. 7 and 8 show the variation of coupling length with wavelength, for *x*- and *y*-polarized light respectively. Comparing Figs. 7 and 8, the *y*-polarized light's coupling length is much less than the coupling length of *x*-polarized light. The birefringence is very small for smaller air holes, but the mode coupling is very strong (small coupling length). Large-diameter air holes give small mode coupling and higher birefringence. Hence, the *d/D* value of 0.7 is selected as the best dual-core hexagonal-shaped PCF structure for splitter realization. The coupling length for *x*- and *y*-polarized light at 1.55 μm is listed in Table 3.

IV. DUAL-CORE HEXAGONAL-SHAPED PCF BASED POLARIZATION SPLITTER

A dual-core hexagonal-shaped PCF based polarization splitter is implemented. From the simulation results, it is concluded that, the value $d/D = 0.7$ is the optimized structure. It has higher birefringence and very short coupling length. The proposed PCF structure yield the high value of 1.802 $\times 10^{-3}$ for birefringence and 1.0962 mm as coupling length for *x*-polarized light. A coupling length of 0.6974 mm is obtained for *y*-polarized light. The results show that the coupling length of the *y*-polarized light is very much less than that for the *x*-polarized light. Different coupling lengths are obtained for *x*- and *y*-polarized light, because of the high birefringence.

In this work, two solid cores are guiding the light by an index-guiding mechanism. When broadband light is applied at the input, the linearly polarized light beams are transferred through the fiber. Assume that the power transmitted in cores C_1 and C_2 at the input side have values of 1 and 0

TABLE 3. *x*-polarized and *y*-polarized light coupling length at 1.55 μm

	Coupling length				
	$d/D = 0.5$	$d/D = 0.6$	$d/D = 0.7$	$d/D = 0.8$	$d/D = 0.9$
x-polarized light	0.5039 mm	0.6993 mm	1.0962 mm	1.5937 mm	2.3859 mm
y-polarized light	0.4081 mm	0.5048 mm	0.6974 mm	1.1007 mm	1.4982 mm

respectively. As per mode-coupling theory, the light will be completely transferred from one core to another core at the coupling length.

Higher birefringence is required for separating the input into *x*- and *y*-polarized light. In the simulation results, *y*-polarized light gives a lesser coupling length. Therefore, *y*-polarized light will be completely transferred into the other core. Figs. 9 and 10 illustrate the power transfer of *x*- and *y*-polarized light at a wavelength of 1550 nm, for a 3 mm fiber.

Normalized power transmission of *x*-polarized light in cores C_1 and C_2 is illustrated in Fig. 11. First, the light source is connected to core C_1, but the *x*-polarized light is switched to core C_2 at the coupling length of 1.0962 mm. At 1.0962 mm coupling length, it is observed that power transmission in core C_1 is very low and power transmission in core C_2 is large. Again, with the similar length, power transmission of *x*-polarized light will be greater in core C_1 and very much less in core C_2.

Normalized power transmission of *y*-polarized light in cores C_1 and C_2 is shown in Fig. 12, from which it is observed that *y*-polarized light will completely transfer to core C_2 at a coupling length of 0.6974 mm. Again, with the similar distance, it changes to core C_1. At a fiber length of 1.9 mm, the maximum amount of *y*-polarized light is directed to core C_2, while *x*-polarized light is coupled to core C_1. Therefore, for a 1.9 mm fiber the *x*- and *y*-polarized light can be separated, as shown in Figs. 12 and 13 respectively, as long as the length of the PCFs

$$L_{oc} = aL_x = bL_y \tag{4}$$

where a and b are positive integers. For a coupling device, the values of a and b must be the same (either odd or even numbers), whereas for a splitter they must be different.

At 1.9 mm, the maximum amount of *x*-polarized light is transferred in core C_1 and the *y*-polarized light is transferred in core C_2. Therefore, at a fiber length of 1.9 mm,

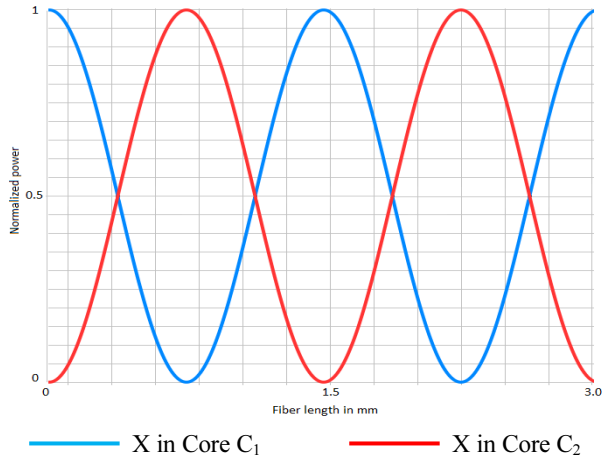

FIG. 9. Normalized power transmission of *x*-polarized light in cores C_1 and core C_2 at 1550 nm.

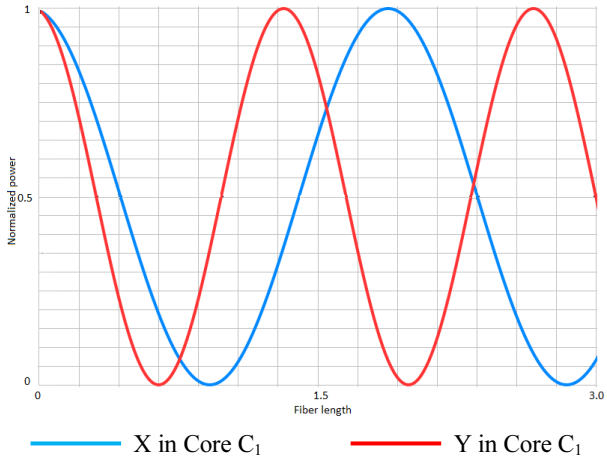

FIG. 11. Normalized power transmission of *x*- and *y*-polarized light in core C_1 at 1550 nm.

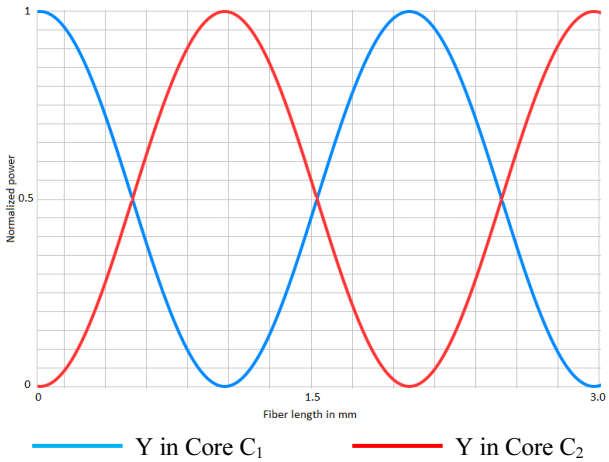

FIG. 10. Normalized power transmission of *y*-polarized light in cores C_1 and core C_2 at 1550 nm.

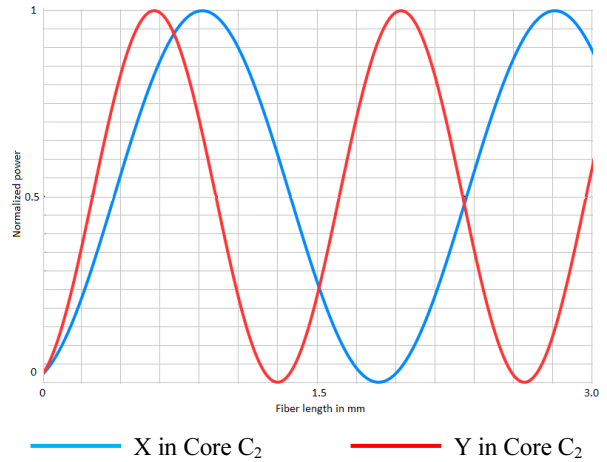

FIG. 12. Normalized power transmission of *x*- and *y*-polarized light in core C_2 at 1550 nm.

the connected light source can be separated as *x*- and *y*-polarized light.

The efficiency of the proposed polarization splitter is measured with the help of the extinction ratio (E_r). For core C_1, the splitting ratio is defined as

$$E_r = 10\log_{10}\frac{y-polarized(light-power)}{x-polarized(light-power)} \quad (5)$$

This splitting ratio indicates the performance of the proposed splitter. The splitting ratio is calculated using Equation. 4 and is shown in Fig. 13. A polarization splitter is realized for 1.9 mm length using the optimized structure with *d/D* ratio 0.7. The result shows that the extinction ratio of this dual-core hexagonal-shaped PCF splitter can give -34.988 dB at 1550 nm wavelength, which is better than -20 dB at wavelengths from 1508 -to- 1589 nm. Its bandwidth in one band gap is about 81 nm.

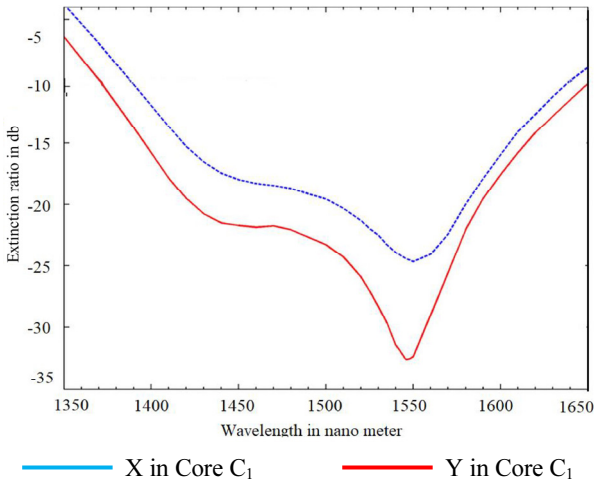

FIG. 13. Extinction ratio of 1.9 mm fiber length versus wavelength, in core C_1.

The proposed splitter gives an improved extinction ratio, compared to existing splitters [20-24]. The comparisons are shown in Table 4.

V. CONCLUSION

In this paper, a dual-core hexagonal-shaped PCF was designed. In addition, its physical properties were analyzed to obtain high birefringence and short coupling length for different values of structural parameters, and were analyzed for a polarization-splitter application. The optimized structure with *d/D* of 0.7 yields a birefringence of 1.802×10^{-3} and a 0.6974 mm coupling length. A 1.9 mm long fiber polarization splitter is realized with a splitting ratio of -34.988 dB at 1550 nm wavelength. Its bandwidth in one band gap is about 81 nm.

REFERENCES

1. W. Su, S. Lou, H. Zou, and B. Han, "A highly nonlinear photonic quasi-crystal fiber with low confinement loss and flattened dispersion," Opt. Fiber Technol. **20**, 473-477 (2014).
2. A. Yasli and H. Ademgil, "Geometrical comparison of photonic crystal fiber-based surface plasmon resonance sensors," Opt. Eng. **57**, 030801 (2018).
3. G. Wang, Z. Wang, and F. Yu, "Design of single-polarization single-mode coupler based on dual-core photonic crystal fiber," Opt. Eng. **55**, 027101 (2016).
4. A. Ibrahim, F. Poulon, F. Melouki, M. Zanello, P. Varlet, R. Habert, B. Devaux, A. Kudlinski, and D. A. Haidar, "Spectral and fluorescence lifetime endoscopic system using a double-clad photonic crystal fiber," Opt. Lett. **41**, 5214-5217 (2016).
5. M. Liu, J. Xiang, and Y. Zhong, "Band structures analysis method of two-dimensional phononic crystals using wavelet-based elements," Crystals **7**, 328 (2017).

TABLE 4. Comparison of conventional splitters with proposed polarization splitter

Scheme	Fiber length	Splitting ratio (bandwidth)	Type of fiber construction
Zhang's scheme [20]	1.7 mm	40 (< -11 dB)	Dual-core PCF with various diameter air holes, higher birefringence
Nahar's scheme [21]	1.055 mm	270 (< -16 dB)	Elliptical shaped dual-core PCF
Chen's scheme [22]	5.9 mm	101 (< -20 dB)	Asymmetric dual-core PCF
Yang's scheme [23]	5 mm	Not mentioned (≤ 20 dB)	Non-birefringent cores with simple structure PCF
Jianhua's scheme [24]	4.72 mm	190 (< -20 dB)	Hybrid dual-core PCF with higher birefringence
Proposed scheme	1.9 mm	81 (< -20 dB)	Dual-core hexagonal-shaped PCF with higher birefringence

6. V. Sharma and R. Sharma, "Design of hybrid photonic crystal fiber with elliptical and circular air holes analyzed for large flattened dispersion and high birefringence," J. Nanophotonics **10**, 026016 (2016).
7. F. Koohi-Kamali, M. Ebnali-Heidari, and M. K. Moravvej-Farshi, "Designing a dual-core photonic crystal fiber coupler by means of microfluidic infiltration," International Journal of Optics and Photonics **6**, 83-96 (2012).
8. Y. Su, H. Zhou, Y. Wang, and H. Shen, "A novel polarization demodulation method using polarization beam splitter (PBS) for dynamic pressure sensor," Opt. Fiber Technol. **41**, 69-73 (2018).
9. L. Gu, L. Liu, S. Hu, A. Zeng, and H. Huang, "Polarization phase-shifting lateral shearing interferometer with two polarization beam splitter plates," Opt. Rev. **24**, 600-604 (2017).
10. Z. Xu, X. Li, W. Ling, P. Liu, and Z. Zhang, "Design of short polarization splitter based on dual-core photonic crystal fiber with ultra-high extinction ratio," Opt. Commun. **354**, 314-320 (2015).
11. J. Li, R. Wang, J. Wang, B. Zhang, and Z. Xu, "Novel polarization splitter based on highly birefringent dual-core photonic crystal fibers with hollow ring defects," Frequenz **68**, 51-57 (2014).
12. Z. Fan, S. Li, Q. Liu, J. Li, and Y. Xie, "Plasmonic polarization beam splitter based on dual-core photonic crystal fiber," Plasmonics **10**, 1283-1289 (2015).
13. H. Chen, S. Li, G. An, J. Li, Z. Fan, and Y. Han, "Polarization splitter based on d-shaped dual-core photonic crystal fibers with gold film," Plasmonics **10**, 57-61 (2015).
14. Q. Liu, S. Li, X. Wang, and M. Shi, "Theoretical simulation of a polarization splitter based on dual-core soft glass PCF with micron-scale gold wire," Chin. Phys. B **25**, 124210 (2016).
15. H. Zou, H. Xiong, Y. Zhang, Y. Ma, and J. Zheng, "Ultra-broadband polarization splitter based on graphene layer-filled dual-core photonic crystal fiber," Chin. Phys. B **26**, 12 (2017).
16. K. S. Hong, S. D. Lim, H. S. Park, and S. K. Kim, "Analysis on transition between index- and bandgap-guided modes in photonic crystal fiber," J. Opt. Soc. Korea **20**, 733-738 (2016).
17. M. P. S. Rao and V. Singh, "Dispersion and nonlinear properties of elliptical air hole photonic crystal fiber," Curr. Opt. Photon. **2**, 525-531 (2018).
18. H. Wu and F. Li, "Negative-refraction effect for both TE and TM polarizations in two-dimensional annular photonic crystals," Curr. Opt. Photon. **2**, 47-52 (2018).
19. G.-J. Jung, J.-H. Kim, and H.-S. Jung, "Ti:$LiNbO_3$ 2×2 optical add/drop multiplexers utilizing acousto-optic effect," J. Opt. Soc. Korea **6**, 27-32 (2002).
20. L. Zhang and C. Yang, "Polarization splitter based on photonic crystal fibers," Opt. Exp. **11**, 1015-1020 (2003).
21. N. K. Nahar and R. G. Rojas, "Coupling loss from free space to large mode area photonic crystal fibers," J. Lightwave Technol. **26**, 3669-3676 (2008).
22. M. Y. Chen, B. Sun, Y. K. Zhang, and X.-X. Fu, "Design of broadband polarization splitter based on partial coupling in square-lattice photonic-crystal fiber," Appl. Opt. **49**, 3042-3048 (2010).
23. L. Zhang, C. Yang, C. Yu, T. Luo, and A. E. Willner, "PCF-based polarization splitters with simplified structures," J. Lightwave Technol. **23**, 3558-3565 (2005).
24. J. Li, J. Wang, R. Wang, and Y. Liu, "A novel polarization splitter based on dual-core hybrid photonic crystal fibers," Opt. Laser Technol. **43**, 795-800 (2011).